Eur. Phys. J. A **23**, 41–48 (2005)
DOI 10.1140/epja/i2004-10068-x

THE EUROPEAN PHYSICAL JOURNAL A

Beta-decay studies of neutron-rich Sc-Cr nuclei

L. Gaudefroy[1], O. Sorlin[1,a], C. Donzaud[1], J.C. Angélique[2], F. Azaiez[1], C. Bourgeois[1], V. Chiste[1], Z. Dlouhy[3], S. Grévy[2], D. Guillemaud-Mueller[1], F. Ibrahim[1], K.-L. Kratz[4], M. Lewitowicz[5], S.M. Lukyanov[6], I. Matea[5], J. Mrasek[3], F. Nowacki[7], F. de Oliveira Santos[5], Yu.-E. Penionzhkevich[7], B. Pfeiffer[4], F. Pougheon[1], M.G. Saint-Laurent[5], and M. Stanoiu[1]

[1] Institut de Physique Nucléaire, IN2P3-CNRS, F-91406 Orsay Cedex, France
[2] LPC, ISMRA, F-14050 Caen Cedex, France
[3] Nuclear Physics Institute, AS CR, CZ-25068, Rez, Czech Republic
[4] Institut für Kernchemie, Universität Mainz, D-55128 Mainz, Germany
[5] GANIL, B.P. 5027, F-14076 Caen Cedex, France
[6] FLNR, JINR, 141980 Dubna, Moscow region, Russia
[7] IReS, IN2P3-CNRS, Université Louis Pasteur, BP 28, F-67037 Strasbourg Cedex, France

Received: 20 April 2004 / Revised version: 28 June 2004 /
Published online: 19 November 2004 –
Communicated by D. Guerreau

Abstract. The neutron-rich nuclei $^{57,58}_{21}$Sc, $^{58-60}_{22}$Ti, $^{60-63}_{23}$V, $^{62-66}_{24}$Cr have been produced at Ganil via interactions of a 61.8 A MeV ^{76}Ge beam with a ^{58}Ni target. Beta-decay studies have been performed using combined β- and γ-ray spectroscopy. Half-lives have been determined and β-decay schemes are proposed for ^{58}Ti, ^{61}V and ^{62}Cr. From these studies, new hints for the existence of β-decaying isomers in ^{60}V and in ^{62}Mn are provided. These results are compared to shell model calculations. The role of the $\pi f_{7/2}$-$\nu f_{5/2}$ proton-neutron interaction is examined through its influence on the lifetime values.

PACS. 27.50.+e $59 \leq A \leq 89$ – 23.40.-s β decay; double β decay; electron and muon capture – 21.60.Cs Shell model

1 Introduction

The study of nuclei below the semi-magic nucleus ^{68}Ni is interesting for several reasons. Among these, new shell/subshell closures are foreseen at $N = 32/34$ and $N = 40$. However, their emergence depends strongly on competing effects which are hitherto very model-dependent. On the one hand, a weakening of the spin-orbit surface term is predicted for very neutron-rich nuclei as their surface is expected to be more diffuse [1]. Consequently, the $g_{9/2}$ orbital would move closer to the next upper orbital, increasing the size of the $N = 40$ gap between the $f_{5/2}$, $p_{1/2}$ and $g_{9/2}$ orbitals. This would make the $^{60}_{20}$Ca$_{40}$ a doubly magic nucleus. On the other hand, the energy difference between the $f_{5/2}$ and $g_{9/2}$ neutron orbitals would be reduced as compared to $^{68}_{28}$Ni$_{40}$ due to the missing proton-neutron spin-flip interaction between the protons in the $f_{7/2}$ shell and the neutrons in the $f_{5/2}$ shell; the $f_{7/2}$ proton orbital being empty in $^{60}_{20}$Ca$_{40}$. Recent shell model calculations predict that this effect would drastically change the ordering of the neutron orbitals, creating new magic numbers at $N = 32$ [2] and $N = 34$ [3]. Experimental evidences of the strenghtening of the $N = 32$ subshell closure have been provided by refs. [4–9]. However, neither the strength of the proton-neutron interaction nor the weakening of the spin-orbit force could be accurately determined. Therefore, the determination of the variation of the energy of the $f_{5/2}$ neutron orbital through an isotonic chain ranging from $Z = 28$ down to $Z = 20$ is of basic importance to disentangle these two effects. This goal may be partially reachable from the β-decay studies which demand only moderate beam intensity as compared to other experimental methods and whose selection rules could favor the study of certain orbitals.

The nuclei in the vicinity of $^{58}_{22}$Ti$_{36}$ comprise neutrons mainly in the fp orbitals and to a minor extent in the $g_{9/2}$ orbital due to the pairing interaction between the fp and g orbitals [10]. The protons lie in the $f_{7/2}$ shell. Consequently, the β-decay schemes are dominated by the strong Gamow-Teller transition $\nu f_{5/2} \rightarrow \pi f_{7/2}$. Therefore, access to the $\nu f_{5/2}$ orbital is naturally favored through β-decay studies.

This paper focuses on the β-decay studies of the neutron-rich isotopes $^{57,58}_{21}$Sc, $^{58-60}_{22}$Ti, $^{61}_{23}$V, $^{62-66}_{24}$Cr,

[a] e-mail: sorlin@ipno.in2p3.fr

aiming to deduce nuclear-structure information from their half-lives and γ-spectroscopy after β-decay. Results are discussed in the framework of shell model calculations. This work is a continuation of ref. [11] in which β-decays of $^{60-63}$V were studied.

2 Experimental procedure

The neutron-rich isotopes ^{57,58}Sc, $^{58-60}$Ti, $^{60-63}$V, $^{62-66}$Cr have been produced at GANIL by the fragmentation of a 61.8 A MeV $^{76}Ge^{30+}$ beam, of mean intensity 1 eμA, onto a ^{58}Ni target of 118 μm thickness. The nuclei of interest were separated by the LISE3 achromatic spectrometer whose magnetic rigity was tuned to optimize the transmission of ^{62}V and ^{64}Cr fragments. The large number of species transmitted after the first magnet was reduced by employing a wedge-shaped Be foil of 221 μm thickness placed in the intermediate focal plane. Analyzed by a second magnet, the unwanted nuclei were stopped in the thick jaws of the slits mounted in the focal plane. It provides an energy loss selection, roughly proportional to A^3/Z^2, reducing the rate of nuclei close to stability. The nuclei transmitted through the spectrometer were identified by means of 3 consecutive 300, 300, 1500 μm silicon detectors. The first two served for the energy loss and time-of-flight measurements. The last one, into which the nuclei were implanted, determines their residual energies. It is segmented into sixteen 3 mm wide, 46 mm height vertical strips. The rate of nuclei implanted was about ten per minute in each strip. Figure 1 shows an energy loss *versus* time-of-flight spectrum obtained for the main setting of the spectrometer in the experiment. The total number of implanted Sc-Cr isotopes is given in table 1. Four Ge detectors were placed around the Si telescope to detect the γ-rays originating from the decay of an isomeric state in the μs range lifetime and the γ-rays emitted up to 1 second after the β-decay. The known delayed γ-rays from isomeric states in ^{60}V (99 and 103 keV) [12], ^{64}Mn (135 keV) [13] and ^{67}Fe (367 keV) [14] have been used to confirm the identification of the transmitted nuclei. In addition to this, a new isomer of 590(130) ns lifetime has been found in ^{59}Ti through the observation of delayed γ-rays with energy of 117(2) keV.

The thick Si detector was used to collect the β-rays following the implantation of a radioactive nucleus. Due to the electronics dead time, β-rays could be detected 100 μs after the implantation of the heavy ion. Each time a nucleus was detected in one of the strips $\#i$, the primary beam was switched off during 1 second to collect the β-particles. These beta-rays were attributed to a precursor nucleus when detected in the same $\#i$ or an adjacent $\#i \pm 1$ strip. About 75% of the β-rays were detected in the same strip as the precursor nucleus. Additional 20% were detected in the adjacent ones. They correspond to cases where the precursor nucleus was implanted at the border of two strips. With an energy threshold of individual strips of 50 keV, the β-efficiency is found to be very similar for all nuclei ($\epsilon_\beta \simeq 90(5)\%$).

The fitting procedure to determine the half-lives includes five parameters: the half-lives of the mother, the daughter and grand-daughter nuclei, the β-efficiency and the background rate over the 1 second collecting time. The daughter and grand-daughter half-lives were known in most of the cases. The β background is due to the decay of long-lived nuclei produced by filiations. Its contribution has been determined over the whole experiment by taking the β-rays anti-correlated in position with the implantation of a nuclei in strip $\#i$, *e.g.* detected in all strips but the $\#i$, $i \pm 1$ ones (procedure described in detail in ref. [16]). Beta-decay time spectra correlated with the implantation of neutron-rich Sc, Ti and Cr nuclei are shown in fig. 3. The results of the V chain have been published in [11]. In the cases where the spectra contain low statistics (less than 200 β's), the maximum-likelihood minimization procedure is applied for the determination of the half-lives. For all other cases, a χ^2-fit is used.

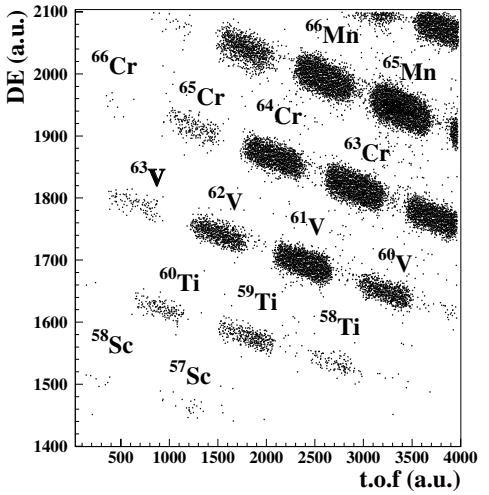

Fig. 1. Identification of the nuclei produced in the experiment by their energy loss (DE) and time of flight (t.o.f), given in arbitrary units.

Table 1. Measured half-lives $T_{1/2}$ in ms for the Sc, Ti, Cr isotopes. The number N of implanted nuclei is indicated in the second column. The half-lives of the daughter nuclei taken into account in the fitting procedure are indicated in the last column.

Isotope	N	$T_{1/2}$	$T_{1/2}$(daughter)
^{57}Sc	26	13(4)	67(25) [15]
^{58}Sc	7	12(5)	59(9)[a]
^{58}Ti	128	59(9)	205(20) [16]
^{59}Ti	424	30(3)	75(7) [15]
^{60}Ti	150	22(2)	40(15)[b]
^{62}Cr	4838	209(12)	92(13) [11]
^{63}Cr	10800	129(2)	275(4) [17]
^{64}Cr	4166	43(1)	89(4) [17]
^{65}Cr	242	27(3)	92(1) [18]
^{66}Cr	9	10(6)	64(2) [18]

([a]) Obtained from the present experiment.
([b]) Taken as a free parameter.

Table 2. Gamma-lines observed in the β-decay of ^{58}Ti, ^{61}V, and $^{62-65}$Cr.

Isotope	γ-rays energies (keV)
^{58}Ti	114
^{61}V	71, 97, 127, 213, 329, 353, 450, 717, 930, 1027, 1144
^{62}Cr	156, 285, 355, 640, 1215
^{63}Cr	250, 879, 1248, 1323, 1670, 1748, 1752, 1890, 2426, 2876, 3175, 3454
^{64}Cr	188
^{65}Cr	272, 1368

Table 2 summarizes the observed γ-lines detected during this experiment. The γ-efficiency $\epsilon_{\beta\gamma}$, gated on the β-rays, has been determined using an additional setting of the spectrometer optimized for the production of ^{65}Fe, ^{67}Co and ^{69}Ni which were implanted in a continuous beam-mode. The known γ-branchings following the β-decay of ^{69}Ni (refs. [19,20]) were used to determine the present $\epsilon_{\beta\gamma}(E)$ efficiency over a wide range of energy. However, its absolute magnitude scales with the (unknown) isomeric content of the $1/2^-$ beta-decaying state in ^{69}Ni, which decays in 74(9)% of cases through the 1298 keV γ-ray [21,22]. We therefore have determined the $\epsilon_{\beta\gamma}$ value at 695 keV from the decay of ^{67}Co (ref. [23]) —which mainly occurs through this γ-ray— to constrain the absolute values of $\epsilon_{\beta\gamma}(E)$. Henceafter, we determined the beam content of ^{69m}Ni to be of about 9%. The $\epsilon_{\beta\gamma}$ value was found to be 6.5 ± 1.3% at 695 keV. The determination of the γ-efficiency has been obtained independently using a ^{152}Eu source located at the Si-strip detector position. A value of ϵ_γ similar to that of $\epsilon_{\beta\gamma}$ has been found, which confirms that the β-efficiency was close to 100%.

3 Results and discussions

The experimental results from the β-delayed γ spectroscopy are presented below. They are compared to shell model calculations. Except when explicitly mentioned, we have calculated the β-decay Gamow-Teller strength functions $S_{\rm GT}$ with the ANTOINE code of Caurier and Nowacki [24,25]. The half-lives have been subsequently deduced using the calculated $S_{\rm GT}$ and the Q_β values of Audi *et al.* [26]. Two sets of interactions, KB3 and KB3G have been used. The KB3 interaction allows to explain the structure of fp nuclei by the use of reaction matrix elements (G-matrix) deduced from a potential determined by fitting the free nucleon-nucleon scattering data [27]. KB3G extends the KB3 interaction and allows to treat properly the gap $N = Z = 28$. [28]. For both interactions a $^{40}_{20}$Ca$_{20}$ inert core has been used. The full fp space was available for protons and neutrons. In this mass region, the β-decay pattern is dominated by the $\nu f_{5/2} \rightarrow \pi f_{7/2}$ Gamow-Teller transition. The first-forbidden transition $\nu g_{9/2} \rightarrow \pi f_{7/2}$ would start to operatate as the $\nu g_{9/2}$ orbital is getting filled. However, its intensity is expected to be by far weaker than the GT ones. Therefore, the $\nu g_{9/2}$ shell has not been included to calculate the β-decay scheme. It would in addition render the calculations hardly tractable. When this orbital is empty —in principle below $N = 40$— the limitation to the fp valence space is sound. We made calculations in the fpg valence space to determine the occupation probability of the $g_{9/2}$ orbital in the mother nucleus when approaching $N = 40$ in the Ti, V and Cr isotopic chains. It is found that pairing correlations already shift up few nucleons into the $g_{9/2}$ shell from the fp orbitals at $N = 38$. For instance, the mean number of neutrons in the $g_{9/2}$ shell in $^{62}_{24}$Cr$_{38}$ is 1.7, that in $^{60}_{22}$Ti$_{38}$ is 1.5. This amount is enhanced as the spacing between the neutron $f_{5/2}$ and $g_{9/2}$ orbitals is reduced. This is found to be the case from the release of the $\pi f_{7/2}$-$\nu f_{5/2}$ interaction as the protons are removed from Ni to Ti, which eventually provokes the crossing of the $f_{5/2}$ and $g_{9/2}$ orbitals as shown in fig. 6 of ref. [11].

The consequences of the limitation to the fp space on the calculated β-decay strength $S_{\rm GT}$ and on the β-decay half-life could be qualitatively estimated as follows: the $g_{9/2}$ neutrons contribute weakly to the β-decay strength and not through Gamow-Teller transitions, except at high excitation energy through $\nu g_{9/2} \rightarrow \pi g_{9/2}$. The $g_{9/2}$ neutrons could be considered as "spectators" in the present β-decay process. By using a restricted valence space, we assume that the neutrons are confined in the fp orbits and that the initial wave functions have pure fp content. Consequently the overlap of the initial and final wave functions (mainly $\pi f_{7/2}$) is larger than in reality. Then, we overestimate the $S_{\rm GT}$ values and calculate shorter half-lives $T_{1/2}$ when restricting the calculations in the fp space. We remind that $T_{1/2}$ can be expressed as an integral of the β-decay strength $S_{\rm GT}$ over the excited states E^* in the daughter nucleus as follows:

$$1/T_{1/2} \simeq \int_0^{Q_\beta} S_{\rm GT}(E^*)(Q_\beta - E^*)^5 \, {\rm d}E^*$$

To some extent, the discrepancy between the calculated lifetime in the fp space and the experimental value should reflect the amount of $g_{9/2}$ in the wave function and subsequently the occupation of the $g_{9/2}$ orbital[1] By comparing experimental and calculated $T_{1/2}$ in the Sc to Cr nuclei (table 3), it seems that the calculated values become gradually shorter than experiment as one approaches the $N = 40$ subshell closure. However, other parameters like the —not well known— Q_β value have dramatic influence on the lifetime value as shown in table 3.

As mentioned above, the strength of the $\pi f_{7/2}$-$\nu f_{5/2}$ interaction influences the half-life values from the fact that the spacing between the neutron $f_{5/2}$ and $g_{9/2}$ orbitals —and hereafter the occupation of the neutron $g_{9/2}$ orbital— changes. To estimate this effect, we have made a parameter study for the ^{58}Ti isotope using the Ragnarsson and Sheline [29] mean field in which the energy of the $f_{5/2}$ orbital has been varied. The Q_β values are taken from

[1] This method could be applied in the $N = 20$ region to infer the amount of the intruder $f_{7/2}$ orbital when reaching the so-called island of inversion.

Table 3. Calculated half-lives $T_{1/2}$ in ms are given in the third and fourth column using KB3 and KB3G interactions, respectively. These half-lives vary as a function of the Q_β values, taken within the experimental uncertainties. The fifth column shows the experimental values, for comparison.

Isotope	Q_β (MeV)	$T_{1/2}^{\rm KB3}$	$T_{1/2}^{\rm KB3G}$	$T_{1/2}^{\rm meas.}$
$^{57}_{21}Sc_{36}$	12.03	22	27	13(4)
	12.86	16	18	
	13.69	11	13	
$^{58}_{21}Sc_{37}$	14.53	16	13	12(5)
	15.59	10	8	
	16.65	7	5	
$^{58}_{22}Ti_{36}$	8.70	84	60	59(9)
	9.44	54	39	
	10.18	36	26	
$^{59}_{22}Ti_{37}$	11.09	29	29	30(3)
	11.85	21	21	
	12.61	15	15	
$^{60}_{22}Ti_{38}$	10.00	20	19	22(2)
	10.93	13	12	
	11.86	8	8	
$^{61}_{23}V_{38}$	12.34	17	16	41(1)
	12.82	14	13	
	13.30	11	10	
$^{62}_{24}Cr_{38}$	7.22	102	132	209(12)
	7.62	794	100	
	8.02	62	76	

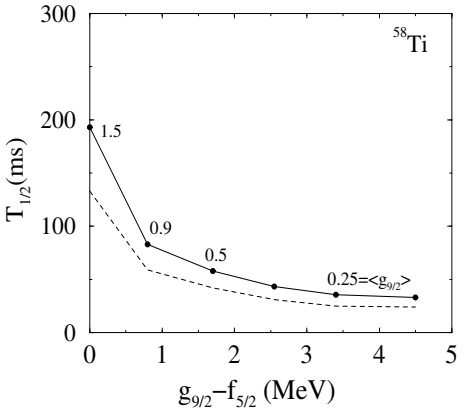

Fig. 2. Evolution of calculated half-life of ^{58}Ti as a function of the energy difference between the neutron $f_{5/2}$ and $g_{9/2}$ orbitals assuming a Q_β value of 9.44 MeV (full line) and 10.18 MeV (dashed line). These Q_β values correspond to the mean and upper limits of Audi *et al.* [26], respectively. The corresponding mean occupation values of the neutron $g_{9/2}$ orbital $\langle g_{9/2}\rangle$ are written on top of the solid curve. The experimental half-life of ^{58}Ti is 59(9) ms.

Audi *et al.* [26]. This study has been made for ^{58}Ti which is predicted to be spherical both in the FRDM [30] and HFB-D1S [31] calculations. The *spherical* wave functions have been deduced for various single-particle energy differences between the neutron $f_{5/2}$ and $g_{9/2}$ orbitals. The Lipkin-Nogami approximation is applied to calculate the pairing correlations. The QRPA of Möller and Randrup has been used to calculate $S_{\rm GT}$ and β-decay half-lives, which are reported in fig. 2. This model is much less time-consuming than shell model calculations and allows to make a parameter study in a large model space but the quadrupole deformation has to be fixed *a priori*. The ^{58}Ti nucleus β-decays mainly through a single transition at low energy, as will be confirmed by the experiment in the following. When the spacing between the neutron $f_{5/2}$ and $g_{9/2}$ orbitals is reduced, the half-life is increased, as shown in fig. 2. This arises from the fact that neutrons are shifted up in the $g_{9/2}$ orbital (due to the pairing interaction) which lowers the amount of GT strength. From the comparison between the calculated and measured lifetime of 59(9) ms (presented in the text below), we could infer that the $f_{5/2}$-$g_{9/2}$ neutron single-particle energy spacing could be as low as 1 MeV in $^{58}_{22}Ti_{36}$ considering the presently large uncertainty on its Q_β value. The experimental results for all studied Sc-Cr isotopes are presented below.

Sc isotopes

^{57,58}Sc: In spite of the very weak statistics, half-lives can be deduced for the first time for these two isotopes (fig. 3) but no γ-ray has been detected.

Ti isotopes

^{58}Ti: A total of 128 nuclei have been implanted. The present half-life value of 59(9) ms is in accordance with the one of 47(10) ms measured in ref. [15]. We see two γ lines at 114(2) keV and 880(1) keV in the β-gated γ spectrum of ^{58}Ti. The 880(1) keV one was observed by Mantica *et al.* [7] in the β-decay of the daughter nucleus ^{58}V. It was attributed to the 2^+ energy of ^{58}Cr. We find that 80(10)% of the decay of ^{58}Ti occurs through the 114(2) keV transition. This transition could either be a member of a γ-cascade from a high-lying excited state in ^{58}V, or correspond to the direct decay of a 114(2) keV level to the ground state. We rather favor the second hypothesis, since we do not see any other γ-line in the spectrum. Given the evolution of $\epsilon_{\beta\gamma}$ value as a function of the γ-ray energy, a γ-ray of up to 2 MeV with a β-branching of $I_\beta = 50\%$ would have been seen, if present. However, this value of 80(10)% is an upper limit of the direct feeding to the 114(2) keV level. Taking the experimentally measured half-life of 59 ± 9 ms and Q_β of 9440(740) keV from Audi *et al.* [26], a $\log(ft)$ value of 3.9(3) is deduced for the 114(2) keV level, which is of the order of the typical allowed GT-transition. The ground-state spin value of the even-even ^{58}Ti nucleus is 0^+. Therefore, the β-decay selection rules imply that the 114(2) keV level in ^{58}V has a 1^+ spin value. This 114(2) keV γ-ray is emitted promptly after the β-decay of ^{58}Ti. This implies a spin difference of $\Delta J \leq 1$ between the corresponding level and the ground state of ^{58}V of which the spin is therefore 0, 1 or 2. In case of a larger spin difference as $\Delta J = 2$, the 114 keV state in ^{58}V would have been an $E2$ or $M2$ isomer, as the one observed in ^{60}V [11].

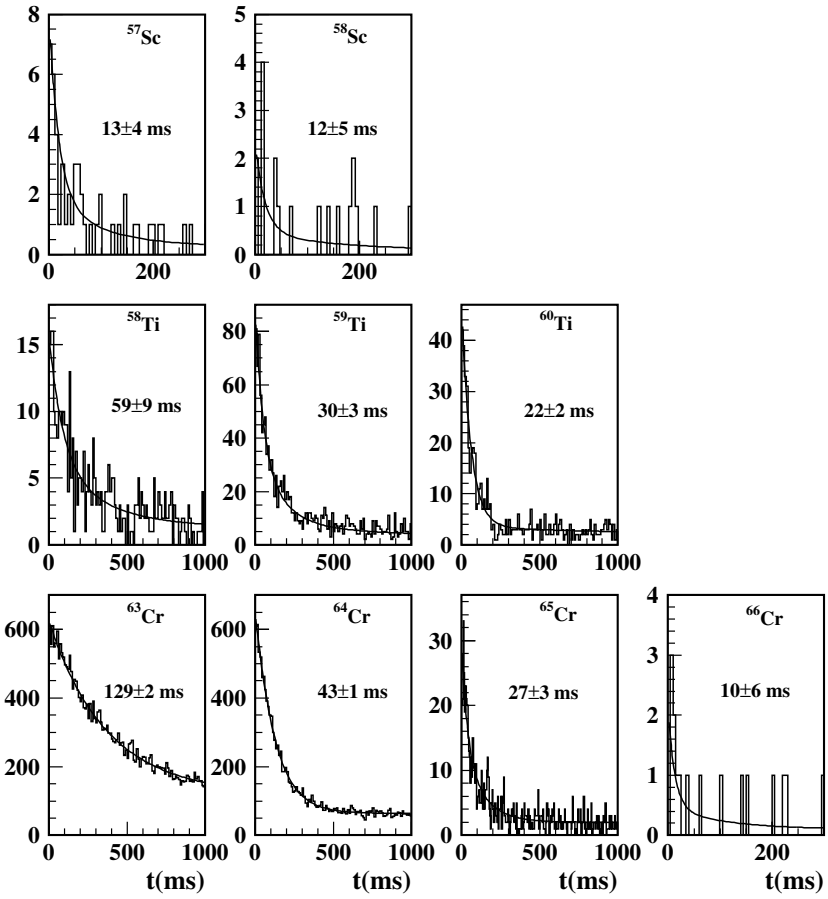

Fig. 3. Beta-decay curves of ^{57,58}Sc, $^{58-60}$Ti and $^{63-66}$Cr. The corresponding half-lives $T_{1/2}$ are included for each isotope.

Shell model calculations give a 2^+ ground state and a 1^+ first excited state in ^{58}V. The energy of the 1^+ is 179 keV with the KB3 interaction, and 46 keV with the KB3G ones. The experimental value lies in the middle. The calculations of β GT-strength function and the β-feedings I_β in the decay of ^{58}Ti points towards an important feeding of the first 1^+ state: 70% with the KB3 interaction and 60% with KB3G, which is in good agreement with the experimental value of 80(10)%. The calculated half-life value (see table 3) also agrees with the experiment.

^{59,60}Ti: The present half-life value of ^{59}Ti, $T_{1/2}$ = 30(3) ms, is more accurate than the value of 58(17) ms determined in ref. [15]. As mentioned above, we have found a γ-isomer at 117(2) keV of 590(130) ns in ^{59}Ti. The half-life value of ^{60}Ti is determined for the first time. That of the daughter nucleus was found to be 40(15) ms as discussed in ref. [11]. Mean values of the calculated half-lives of ^{59,60}Ti are somewhat shorter than the experimental values (table 3), but agree within the uncertainties provided by the Q_β limits. We estimate from shell model calculations that in $^{58}Ti_{36}$, the occupation of the $g_{9/2}$ orbital is 0.5. It rises to 1.5 in $^{60}Ti_{38}$.

These $T_{1/2}$ values agree with those of ref. [32] obtained at GANIL, after the present experiment, from the fragmentation of a ^{86}Kr beam. In this reference two γ-isomers of $E2$ and $M2$ multipolarities have been reported in ^{59}Ti, with energies of 117(2) keV (which agrees with ours) and 699(1) keV (which originates from the decay of a positive parity state), respectively. The same experiment also reports an $E2$ isomer in ^{61}Ti. The presence of $E2$ isomers in ^{59,61}Ti points towards a sequence of levels with spin values of $5/2^-$-$1/2^-$ which could arise from the neutron $f_{5/2}$ and $p_{1/2}$ orbitals. Moreover, Mantica *et al.* [9] reported that the β-decay strength of ^{55}Ti was shared among five states in ^{55}V, which was interpreted as resulting from a mixed configuration between $f_{5/2}$ and $p_{1/2}$ orbitals in the ^{55}Ti ground state. However, shell model calculations using the GXPF1 interaction did not reproduce the decay scheme of ^{55}Ti. The calculated g.s. spin value was $1/2^-$, whereas the experiment rather points to a $5/2^-$ configuration.

We have performed shell model calculations with the KB3 and KB3G interactions to see the evolution of structure in the titanium chain. There, the ordering of the neutron orbitals above $N = 28$ is $p_{3/2}$, $p_{1/2}$ and $f_{5/2}$, leading to two subshell closures at $N = 32$ and $N = 34$. Even though a $5/2^-$-$1/2^-$ doublet is present at low energy along the Ti chain, its composition varies as the neutron number increases. In ^{55}Ti, both the KB3 and KB3G interactions find a mixture of $f_{5/2}$ and $p_{1/2}$ configurations in the $5/2^-$

and $1/2^-$ states, whereas they become almost pure $f_{5/2}$ in ^{59}Ti. The KB3 and KB3G calculations for ^{55}Ti lead to g.s. spins of $1/2^-$ and $5/2^-$, respectively. However none of these interactions fully reproduce the observed β-decay pattern in ^{55}Ti [9].

V isotopes

^{61}V: Results from the β-decay studies of the neutron-rich $^{60-63}$V isotopes have been reported in ref. [11]. However the detailed $\beta\gamma$-spectroscopy of ^{61}V was not exploited. A total of 5858 nuclei ^{61}V were implanted. The sum of all the detected γ-transitions amounts to 35(10)% of the β strength. The missing strength could occur to the g.s. or/and to high-energy states. Given the present β-γ efficiency as a function of the energy of the photon and the number of implanted nuclei, we estimate that 2.5 MeV γ-rays originated from levels fed by $I_\beta \leq 10\%$ would have not been seen. This limit would increase if the high-energy excited states decay through several γ-transitions with weak intensities for each. Shell model calculations predict that the β-strength is fragmented over 10 levels in ^{61}Cr with about 10% intensity each. These levels are almost regularly spaced between 500 keV and 3 MeV. About 30% of the decay occurs below 1.5 MeV, which might correspond to the part we see in our analysis. These decay branch would correspond to the decay of the calculated $3/2^-$ state in ^{61}V to the three components $1/2^-$, $3/2^-$ and $5/2^-$ corresponding to single-particle configurations of a neutron in $f_{5/2}$ in ^{61}Cr. In addition to this, some states corresponding to the recoupling to the 2^+ energy of the ^{60}Cr core are also present at low energy. This is part of the reason why the β-decay strength is fragmented over several states. Given our present statistics, no $\gamma\gamma$ coincidence has been found. A tentative (partial) β-decay sheme of ^{61}V, based on the energy of the γ-rays and their intensities, is presented in fig. 4.

The expected configuration of $^{61}_{23}V_{38}$ is $f_{7/2}$: $\pi[321]3/2^-$ for a wide range of quadrupole deformation parameter (see, for instance, fig. 7 in [16]). For $^{61}_{24}Cr_{37}$, the ground-state configuration could either be $f_{5/2}$: $\nu[303]5/2^-$ or $p_{1/2}$: $\nu[301]1/2^-$. The GT selection rules strongly favor $\nu f_{5/2} \rightarrow \pi f_{7/2}$ transitions. From the fact that we probably find a feeding of the ^{61}Cr ground state, its configuration is likely to be $\nu[303]5/2^-$. Furthermore, the observed excited levels of ^{61}Cr should have J^π values of $1/2^-$, $3/2^-$, or $5/2^-$ from the β-decay selection rules.

Cr isotopes

^{62}Cr: The present half-life of ^{62}Cr value, $T_{1/2} = 209(12)$ ms, is in accordance with $T_{1/2} = 187(15)$ ms measured in ref. [15]. We confirm that the fit of the decay curve can be achieved only when attributing a short half-life ($T_{1/2} = 92(13)$ ms) to the daughter nucleus ^{62}Mn. This value differs significantly from the measured half-life of $T_{1/2} = 671(5)$ ms [17] obtained from the β-decay

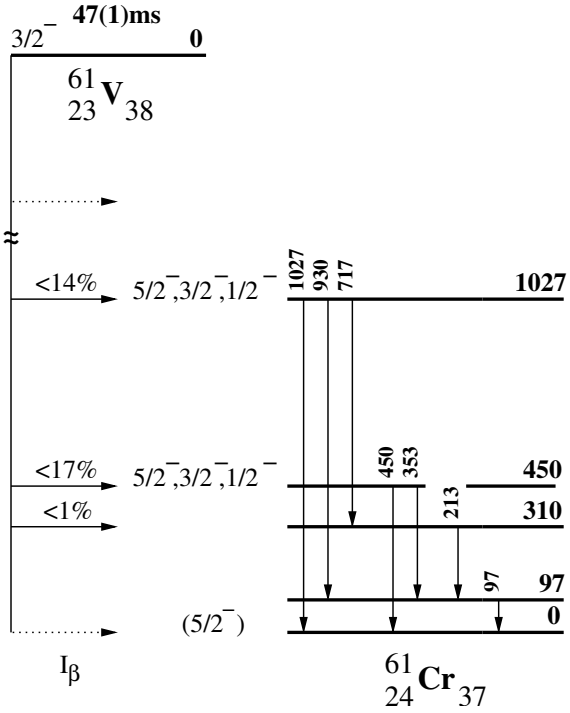

Fig. 4. Tentative decay scheme of $^{61}_{23}V_{38}$.

of ^{62}Mn at CERN/ISOLDE. A long half-life value was also found in the work of Runte *et al.* [33] who suggested a 3^+ spin for the ground state of ^{62}Mn. The combination of these experimental results points to the existence of two beta-decaying states in ^{62}Mn, a long-lived one with $T_{1/2} = 671(5)$ ms [17] and a shorter one with $T_{1/2} = 84(10)$ ms [15] populated in the β-decay of ^{62}Cr. As discussed in ref. [11], the short component probably corresponds to a low spin value since it is fed in the decaying state of the ^{62}Cr whose spin is 0^+. We cannot determine which of these β-decaying states is the ground state. The energy of the short-lived state will be denoted as y in the following; y being of order of hundreds of keV and positive if this level corresponds to the excited state.

In the β-decay of ^{62}Cr, two γ-lines at 355(2) and 285(2) keV are found to be in coincidence. The cross over transition at 640(2) keV is also observed. We, therefore, deduce the existence of a 1^+ state at $640 + y$ keV which is fed with $I_\beta \simeq 25\%$. The intensity of the 355(2) keV line (written in parentheses after the energy of the transition in fig. 5) is found to be 15% smaller than that of the 285(2) keV line. This indicates that an additional β-decay branch decays to the 285(2) keV state. The observed 1215(2) keV γ-line, of $I_\gamma = 15\%$, could account for this missing intensity. It is therefore tentatively placed above the 285(2) keV state, providing a level at $1500 + y$ keV with $I_\beta = 3\%$. It is found that the γ-lines mentioned above are followed by a short β-decay component. We therefore connect these γ-rays to this short-lived state, as shown in fig. 5.

Since we do not see any other γ-line in the ^{62}Cr decay, we deduce that the short-lived β-decaying state is fed by about 73(5)%. This feeding corresponds to a $\log(ft)$ value

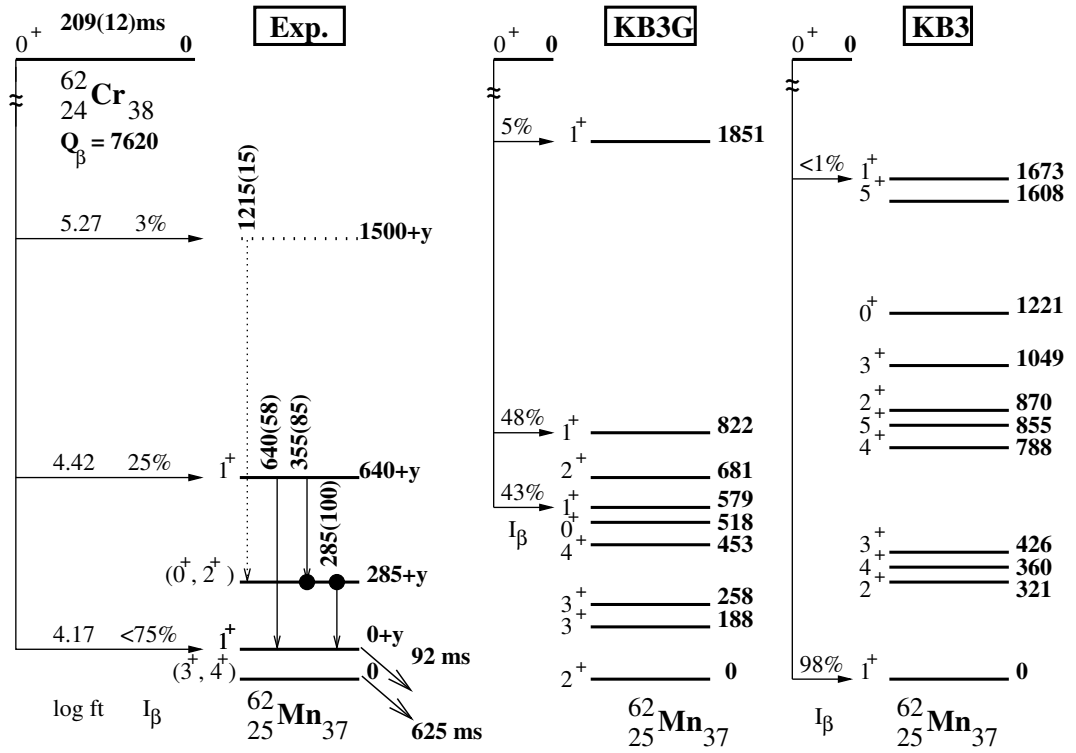

Fig. 5. The experimental β-decay scheme of $^{62}_{24}Cr_{38}$ (left) is compared to the ones calculated with the shell model using the KB3G and KB3 interactions. Beta-feeding intensities I_β and $\log(ft)$ values are indicated for each transitions. Values in parentheses following the energy of the γ-ray transitions correspond to the γ-intensities relative to that of the 285 keV transition (which has been taken to 100).

of 4.2(2), in accordance with an allowed GT transition. The short-lived β-decaying state has therefore probably a 1^+ spin-parity value. We observe a γ-line at 815(2) keV, which has been attributed to the decay of ^{62}Mn from its time-evolution pattern. Since it was not observed by Runte *et al.* [33], we deduce that it is selectively fed from decay of the 1^+ state of ^{62}Mn.

In order to explain the existence of a β-isomer in ^{62}Mn, an important spin and/or a small energy differences with the lower energy states is required. Runte *et al.* [33] suggested a 3^+ spin for ^{62}Mn to account for the feeding of 2^+ and 4^+ excited states in ^{62}Fe. This provides a small spin value difference ($\Delta J = 2$) with respect to the 1^+ state mentioned above. It is therefore hardly conceivable to obtain a β-isomer between these two states, even for very small energy differences. The situation is rather puzzling, and further experimental investigations should be done to clarify the low-energy part of the ^{62}Mn level scheme. We also note that intruder configurations, originating from the filling of the ν $g_{9/2}$ orbital could also account for the presence of a β-isomer.

We have performed SM calculations for comparison to the experimental decay scheme of fig. 5. As mentioned above, the measured lifetime of ^{62}Cr is longer than calculated within the fp valence space. This difference could be traced back from the fact that about 1.7 among 6 neutrons are predicted to be shifted from the $f_{5/2}$ orbital to the intruder $g_{9/2}$ orbital. This would reduce the amount of the GT strength $\nu f_{5/2} \rightarrow \pi f_{7/2}$, henceafter enhancing the lifetime value by a factor 6/4.3. Energies and spins of the ^{62}Mn levels were calculated using the KB3 and KB3G interactions and the fp valence space, as for ^{58}Ti. With the KB3 interaction, the calculated g.s. of ^{62}Mn is 1^+, and states 3^+, 4^+ are present about 400 keV above. The β-strength almost exclusively occurs to the ground state. The calculation with the KB3G interaction provides an inversion between the 1^+ and 3^+, 4^+ levels but none of these two is the ground state. The β-strength is shared equally between two levels. The experimental β-decay scheme is almost intermediate between the two calculated ones.

In addition to what is found in the present work, the existence of an $E2$ γ-isomer of 101(10) ns lifetime which decays through a 113 keV γ-ray was observed by Daugas *et al.* [12]. Since this γ-ray is not observed in the β-decay experiment, its spin value is not 1^+. However, we cannot place this state in the present level scheme unambiguously.

^{63}Cr: The present half-life value, $T_{1/2} = 129(2)$ ms, agrees with $T_{1/2} = 113(16)$ ms obtained in ref. [15]. Many γ-rays above 1.5 MeV are seen in the β-gated γ-delayed spectrum of ^{63}Cr (see table 2). This indicates a large feeding of the high-energy states in the decay of ^{63}Cr. Due to weak statistics, no γ-γ coincidence could be made. We observe only half of the intensity of the β-decay through γ-rays and therefore cannot establish a decay scheme for this nucleus. This could be due to a lack of statistics, but also to a high direct β-feeding to the ground state of ^{63}Mn.

When reaching $N = 40$ and above, the use of the KB3 and KB3G interactions become inappropriate. We therefore use the deformation-dependent QRPA calculations to calculate the β-decay pattern of $^{63}Cr_{39}$. At a fairly large quadrupole deformation parameter $\epsilon_2 \simeq 0.28$, QRPA calculations provide good agreement with the experimental β-strength and half-life. About 45% of the β-strength feed the g.s. of ^{63}Mn and $\simeq 25\%$ feed an exited state at 3.9 MeV, with respective $\log(ft)$ values of 4.95 and 4.33. The calculated half-life is $T_{1/2} = 129$ ms.

^{64}Cr: The present half-life value, $T_{1/2} = 43(1)$ ms is more accurate than $T_{1/2} = 44(12)$ ms obtained in ref. [15]. In the decay of $^{64}_{24}Cr_{40}$, we observe only one γ-line at 188(2) keV which accounts for 17% of the β-strength. Given the presently weak statistics, it is possible to miss part of the β-decay strength which would proceed through high-energy states and γ-decay via various branchings.

^{65,66}Cr: Half-life values of 27(3) ms and 10(6) ms are found for ^{65}Cr and ^{66}Cr, respectively. In the β-decay of ^{65}Cr, two γ-lines are tentatively assigned at 272(2) and 1368(2) keV. In addition to this, the 364(2) keV line which belongs to the decay of the daughter nucleus ^{65}Mn is observed in about 50% of the cases. This value is very similar to the feeding of 54(2)% deduced for this line from the direct β-decay of ^{65}Mn. This shows that the β-decay of ^{65}Cr stays in the $A = 65$ chain and scarcely occurs through β-delayed neutron emission to ^{64}Mn. Otherwise the intensity of the 364(2) keV line in the ^{65}Cr decay would have been much weaker. QRPA calculations find β-delayed neutron emission probablilities P_n lower than 10% for a large set of deformation parameters ranging from $\epsilon_2 = 0.0$ to $\epsilon_2 = 0.26$. Moreover the experimental half-life of 27(3) ms is shorter than the calculated values for a large range of deformation parameters; $T_{1/2} = 67$ ms for $\epsilon_2 = 0$ and $T_{1/2} = 98$ ms for $\epsilon_2 = 0.26$. This could be accounted for by an effect of Q_β value and/or by a shift in energy of the GT strength. Also, we estimate that the first forbidden transitions could shorten the half-lives values above $N = 40$ by about 20%.

4 Conclusion

Beta-decay studies of neutron-rich ^{57,58}Sc, $^{58-60}$Ti, ^{61}V and $^{62-66}$Cr have been achieved using combined β- and γ-ray spectroscopy. Half-lives of ^{57,58}Sc, ^{60}Ti and ^{65,66}Cr are determined for the first time, whereas half-lives of the remaining nuclei are measured with better accuracy as compared to previous studies. Decay schemes are proposed for ^{58}Ti, ^{62}Cr and partly for ^{61}V. They are compared to shell model predictions in the fp valence space using the KB3 and KB3G interactions. Both calculated β-intensities and half-lives are in relatively good agreement with experiment. It is found that the $\nu f_{5/2} \rightarrow \pi f_{7/2}$ GT transition dominates the β-decay pattern. However, the calculated lifetimes in the restricted fp space become gradually shorter than experimental values when approaching a neutron number $N = 40$. This is inferred from the fact that the pairing effect already shifts up neutrons from the $\nu f_{5/2}$ to the $\nu g_{9/2}$ shell already before reaching $N = 40$. This reduces (increases) the Gamow-Teller strength (lifetime) accordingly in the ^{62}Cr where about 1.7 neutrons lie in the $\nu g_{9/2}$ shell. The occupation of the $\nu g_{9/2}$ shell by pair scattering depends strongly on the energy difference between the single particle $\nu f_{5/2}$ and $\nu g_{9/2}$ orbitals. This spacing is very sensitive to the $\pi f_{7/2}$-$\nu f_{5/2}$ interaction which shifts downward the $\nu f_{5/2}$ orbital by some MeV when going from the $N = 40$ Ca to the Ni isotones. The present study does not permit to draw quantitative conclusion about the strength of this proton neutron interaction and the occupation of the $\nu g_{9/2}$ shell since the results are strongly Q_β dependent. However, the description of the role of this interaction in the β-decay process has been described. Better measurements of the atomic masses —and herafter determination of the Q_β values— in this mass region would enable to deduce more quantitive insights.

References

1. J. Dobaczewski *et al.*, Phys. Rev. Lett. **72**, 981 (1994).
2. M. Honma *et al.*, Phys. Rev. C **65**, 061301(R) (2002).
3. T. Otsuka *et al.*, Phys. Rev. Lett. **87**, 082502 (2001).
4. A. Huck *et al.*, Phys. Rev. C **31**, 2226 (1985).
5. J.I. Prisciandaro *et al.*, Phys. Lett. B **510**, 17 (2001).
6. R.V.F. Janssens *et al.*, Phys. Lett. B **546**, 55 (2002).
7. P.F. Mantica *et al.*, Phys. Rev. C **67**, 014311 (2003).
8. D.E. Appelbe *et al.*, Phys. Rev. C **67**, 034309 (2003).
9. P.F. Mantica *et al.*, Phys. Rev. C **68**, 044311 (2003).
10. O. Sorlin *et al.*, Phys. Rev. Lett. **88**, 092501 (2002).
11. O. Sorlin *et al.*, Eur. Phys. J. A **16**, 55 (2003).
12. J.M. Daugas, PhD Thesis, Université de Caen, GANIL-T 99 05 (1999).
13. R. Grzywacz *et al.*, Phys. Rev. Lett. **81**, 766 (1998).
14. M. Sawicka *et al.*, Eur. Phys. J. A **16**, 51 (2003).
15. O. Sorlin *et al.*, Nucl. Phys. A **669**, 351 (2000).
16. O. Sorlin *et al.*, Nucl. Phys. A **632**, 205 (1998).
17. M. Hannawald *et al.*, Phys. Rev. Lett. **82**, 1391 (1999).
18. O. Sorlin *et al.*, Nucl. Phys. A **719**, 193c (2003).
19. U. Bosch *et al.*, Nucl. Phys. A **477**, 89 (1988).
20. S. Franchoo *et al.*, Phys. Rev. C **64**, 054308 (2001).
21. W.F. Mueller *et al.*, Phys. Rev. Lett. **83**, 3613 (1999).
22. J.I. Prisciandaro *et al.*, Phys. Rev. C **60**, 054307 (1999).
23. L. Weissman *et al.*, Phys. Rev. C **59**, 2004 (1999).
24. E. Caurier, Shell Model code ANTOINE, IReS, Strasbourg 1989-2002.
25. E. Caurier, F. Nowacki, Act. Phys. Pol. B **30**, 705 (1999).
26. G. Audi *et al.*, Nucl. Phys. A **729**, 337 (2003).
27. T.T.S. Kuo, G.E. Brown, Nucl. Phys. A **114**, 241 (1968).
28. A. Poves *et al.*, Nucl. Phys. A **694**, 157 (2001).
29. I. Ragnarsson, R.K. Sheline, Phys. Scr. **29**, 385 (1984).
30. P. Möller *et al.*, At. Data Nucl. Data Tables **66**, 131 (1997).
31. M. Girod, private communication.
32. I. Matea, PhD Thesis, Université de Caen, GANIL T03 05 (2003).
33. E. Runte *et al.*, Nucl. Phys. A **399**, 163 (1983).